frontiers | Frontiers in Natural Products

TYPE Original Research
PUBLISHED 14 November 2022
DOI 10.3389/fntpr.2022.958425

OPEN ACCESS

EDITED BY
Lisa Pilkington,
The University of Auckland,
New Zealand

REVIEWED BY
Prabodh Satyal,
Aromatic Plant Research Center,
United States
Sundararajan Balasubramani,
Southwest University, China

*CORRESPONDENCE
Jessica Bravo,
jessica.bravo@udp.cl

SPECIALTY SECTION
This article was submitted to Informatics and Computational Methods, a section of the journal Frontiers in Natural Products

RECEIVED 10 June 2022
ACCEPTED 04 October 2022
PUBLISHED 14 November 2022

CITATION
Bruna F, Fernández K, Urrejola F, Touma J, Navarro M, Sepúlveda B, Larrazabal-Fuentes M, Paredes A, Neira I, Ferrando M, Osorio M, Yañez O and Bravo J (2022), The essential oil from Drimys winteri possess activity: Antioxidant, theoretical chemistry reactivity, antimicrobial, antiproliferative and chemical composition.
Front. Nat. Prod. 1:958425.
doi: 10.3389/fntpr.2022.958425

The essential oil from *Drimys winteri* possess activity: Antioxidant, theoretical chemistry reactivity, antimicrobial, antiproliferative and chemical composition

Flavia Bruna[1,2], Katia Fernández[1], Felipe Urrejola[1], Jorge Touma[1], Myriam Navarro[1], Betsabet Sepúlveda[3], María Larrazabal-Fuentes[4], Adrián Paredes[5], Iván Neira[6], Matías Ferrando[2], Manuel Osorio[1,7], Osvaldo Yañez[8,9] and Jessica Bravo[1]*

[1]Laboratorio de Productos Naturales Bioactivos, Centro de Investigación Biomédica, Facultad de Medicina, Universidad Diego Portales, Santiago, Chile, [2]Laboratorio de Hormonas y Biología del Cáncer, Instituto de Medicina y Biología Experimental de Cuyo (IMBECU), CONICET CCT-Mendoza UNcuyo, Mendoza, Argentina, [3]Facultad de Ciencias Químicas y Farmacéuticas, Universidad de Chile, Santiago, Chile, [4]Departamento de Ciencias de los Alimentos y Nutrición, FACSA, Universidad de Antofagasta, Antofagasta, Chile, [5]Laboratorio Química Biológica, Instituto Antofagasta and Departamento de Química, Universidad de Antofagasta, Antofagasta, Chile, [6]Departamento de Tecnología Médica, FACSA, Universidad de Antofagasta, Antofagasta, Chile, [7]Center for Bioinformatics and Integrative Biology, Facultad de Ciencias de la Vida, Universidad Andrés Bello, Santiago, Chile, [8]Center of New Drugs for Hypertension (CENDHY), Santiago, Chile, [9]Facultad de Ingeniería y Negocios, Universidad de las Américas, Santiago, Chile

The Mapuche and their ancestors have used *D. winteri* in traditional medicine. In the present study, the essential oil extract of *D. winteri* leaves (DW_EO) were characterized chemically and biologically to evaluate its pharmacological activity. *In vitro* antioxidant activity was assayed, and antitumor activity was evaluated in non-tumor and tumor-cell culture lines. *Caenorhabditis elegans* was used as a model to evaluate toxicity, and the chemical composition of the essential oil was analyzed by gas chromatography-mass spectrometry. The chemical oil composition was characterized principally of five major terpenes: 4 sesquiterpenes γ-Eudesmol (39.7%), β-Caryophyllene (33.7%), Elemol (25.9%), α-Eudesmol (0.3%) and 1 diterpene Kaunene (0.4%). By quantum calculations, it was determined that all oils have the ability to capture and yield electrons, which is consistent with the moderate antioxidant activity of DW_EO detected *in vitro*. Furthermore, by molecular docking is estimated that these oils can bind to proteins involved in the production of oxygen radicals. Of these proteins,

Abbreviations: EO, essential oil; DW, Drimys winteri; HP, Helicobacter pylori; EC, Escherichia coli; SA, Staphylococcus aureus; CA, Candida albicans; MC, majority compounds; AC, antioxidant capacity; GC–MS, Gas chromatography–mass spectrometry; MIC, minimum inhibitory concentration; HD, hydrodistillation; DW, Drimys winteri; MW, molecular weight; HBA, H-bond acceptors; HBD, H-bond donor; FRAP, ferric-reducing antioxidant power; DFT, Density functional theory.

CYP2C9 could bind energetically, reaching binding energy between −6.8 and −9.2 kCal/mol for the 5 terpenes studied, highlighting among these β-Caryophyllen and γ-Eudesmol. DW_EO has effect against *H. pylori* (MIC 32 μg/ml), *S. aureus* (MIC 8 μg/ml), *E. coli* (MIC 32 μg/ml) and *C. albicans* (MIC 64 μg/ml), β-Caryophyllen and γ -Eudesmol (MIC 64 μg/ml) and could selectively inhibit the proliferation of epithelial tumor cell lines but showed low against *C. elegans* (0.39–1.56 μg mL^{-1}). Therefore, DW_EO may be used as a source of bioactive compounds in novel pharmacological treatments for medical application, agronomics, sanitation, and food.

KEYWORDS

essential oil, antioxidant, citotoxicity, toxicity, antimicrobial, chemical composition, theoretical reactivity

1 Introduction

D. winteri J.R. et G. Forst, commonly called Canelo, is a native tree that is distributed in Latin America, from Brazil to Argentina and Chile (Perez et al., 2007; Russo et al., 2019). In Chile, it is a sacred tree of great social significance for the Mapuche culture, also used as a medicinal plant (Muñoz-Concha et al., 2004; Monsálvez et al., 2010; Neira Ceballos et al., 2012). It is recognized by the Ministry of Health (MINSAL, 2010; Fratoni et al., 2018) as an herbal medicine and the leaf is used in infusions and the bark in cooking to treat various conditions. The infuse is taken to combat coughs and colds, even chronic ones; in parasitosis (worms), stomach disorders, dysentery, and rheumatic pain. Externally (washes, baths, or poultices) it is used to cure various skin conditions (wounds, ulcers, warts, scabies, or allergies) and to treat rheumatic and muscle pain caused by sprains. Folk medicine recommends the infusion as a treatment for different inflammatory diseases, such as asthma, allergy, and bronchitis (Russo et al., 2019).

It is relevant to know and characterize the components present in the Chilean native flora, such as *D. winteri*, to project its use as a botanical source of bioactive compounds with potential applications in industrial areas. Previous research has shown bioactivity of *D. winteri* bark extracts, leaves and seeds (Zapata and Smagghe, 2010), validate its use as an insecticide or repellent to control different insects or pests (Zapata et al., 2010); present a phytotoxic effect against germination and weed growth. (Paz et al., 2013) report an inhibitory effect of polygodial, drimenol and drimendiol are drimane possess antibacterial, antifungal, antifeedant and plant-growth regulatory properties (Zapata and Smagghe, 2010). Muñoz-Concha demonstrated that the yield and composition of EOs vary according to the geographical area, with higher yields and concentration of terpenes and flavonoids in the north-central zone, which are reduced towards the southern zone of Chile (Muñoz-Concha et al., 2004; Goodarzi et al., 2016). Zapata and Smagghe report a very strong repellent activity and toxicity (topical and by fumigation), of EO_S extracted from leaves and bark of *D. winteri*, against an important pest of stored product insects: the red flour beetle, *Tribolium castaneum* (Zapata and Smagghe, 2010). Hernandez y collaborators report an inhibitory effect of *D. winteri* EOs against phytopathogenic fungi such as *Botritys cinerea* (Hernández et al., 2010).

Several authors report that the bioactivity of extracts and EOs of *D. winteri* (Winteraceae), would be caused mainly by the sesquiterpene drimane (drimanial), which structure was elucidated by (Malheiros et al., 2001). Burgos concluded that drimane sesquiterpenoids, from *D. winteri* could be used as a molecular scaffold in the development of drugs for inflammatory vascular diseases (Burgos et al., 2020).

D. winteri seems to be a well-defended plant since it contains a substantial amount of essential oil as well as drimane-type sesquiterpenes, drimendiol, isotadeonal, isodrimeninol and polygodial. Sesquiterpenoids isolated from *D. winteri*, decreases violaceine production in *C. violaceum* and lowers biofilm formation of *Pseudomonas syringae* strains (Monsálvez et al., 2010) (Zapata et al., 2011), demonstrating antifungal activity (Pereira-Torres et al., 2016); there is potential in *D. winteri* bark extract as a possible immunomodulatory and defensive strategy against this oomycete infection in fish. The medicine area (Russo et al., 2019), suggests that the active molecules extracted from *Drimys winteri* can be considered potential candidates to be tested *in vivo* models, alone or in combination with chemotherapy agents, in the treatment of melanoma (Malheiros et al., 2001). Drimanial isolated from the bark of *D. winteri*, exhibited antinociceptive action against acetic acid induced pain.

The objective of this work is to characterize chemically the essential oil obtained from *D. winteri* leaves by means of GC-MS, to describe the antioxidant potential, to study the chemical properties of each compound by Density Functional Theory (DFT) studies and, the antimicrobial and antitumor capacity in cell line and toxicity.

2 Materials and methods

2.1 Collection identification and extraction

The aerial parts of *D. winteri* J.R. et G. Forst, was collected at the beginning of the flowering season in September 2015 from

Curiñanco (39°48′30″ S and 73°14′30″ W) Valdivia, Chile. The plant was identified by Dr. Carlos Valdovinos, and a voucher specimen was deposited at the Herbarium of the Facultad de Ciencias Químicas y Farmacéuticas, Universidad de Chile (N° 22695 SQF). The EO was extracted by water distillation in a Clevenger-type apparatus. The EO was dried over anhydrous sodium sulfate, stored at 4°C and kept under liquid nitrogen as previously described until further analysis (Avello Lorca et al., 2012).

2.2 Antioxidant capacity

2.2.1 Chemical materials

1,1-Diphenyl-2-picrylhydrazyl radical (DPPH), 2,4,6-tris-(2-pyridyl)-s-triazine (TPTZ), (-)-6-hydroxy-2,5,7,8-tetramethylchromane-2-carboxylic acid (Trolox), potassium persulfate ($K_2S_2O_8$), H_2O for HPLC, and monobasic (NaH_2PO_4) and dibasic (Na_2HPO_4) sodium phosphate were purchased from Sigma-Aldrich (St. Louis, MO, United States). Iron (III) chloride hexahydrate ($FeCl_3$ $6H_2O$), iron (II) sulfate heptahydrate ($FeSO_4$ $7H_2O$), hydrochloric acid (HCl), methanol (MeOH), 2, 2′-azino-bis (3-ethylbenzothiazoline-6-sulfonic acid) diammonium salt (ABTS), and EDTA disodium salt were purchased from Merck (Darmstadt, Germany).

2.2.2 Ferric-reducing antioxidant power assay

The FRAP assay was performed using a previously described method (Karadag et al., 2009). It was taken 10 µL of the DW_EO solution at a final concentration of 500 µg ml^{-1} (10 mg EO dissolved in 1 ml absolute EtOH and subsequently diluted to obtain a working solution of 500 µg ml^{-1}) (Karadag et al., 2009; Pinchuk et al., 2012) was mixed with 70 µL of freshly prepared FRAP solution at a ratio of 10:1 (v/v) [300 mM acetate buffer (pH 3.6), 10 mM 2,4,6-tris-(2-pyridyl)-s-triazine (TPTZ) dissolved in 40 mM HCl, and 20 mM $FeCl_3{\cdot}6H_2O$ aqueous solution]. After incubating the solution for 30 min at 37°C, absorbance was measured at 593 nm with a microplate reader (BioTek Synergy HTX Multimodal Kit; Winooski, VT, United States) and the values were interpolated onto a Trolox calibration curve over a concentration range of 0–500 µg ml^{-1}. FRAP results were expressed as milligrams of Trolox equivalents per gram of EO. All experiments were performed in triplicate.

2.2.3 Metal chelating activity (ferrozine)

The chelating activity of DW_EO against iron (II) ions was assayed using the method described by Sudan (Sudan et al., 2014) with some modifications. Briefly, 50 µL of EO at a final concentration of 500 µg ml^{-1} was mixed with 10 µL of 2 mM $FeCl_2$ (prepared in HPLC-grade water). The reaction was started by the addition of 20 µL of 5 mM ferrozine (prepared in HPLC-grade water). The total volume was adjusted to 150 µL with methanol (70 µL). After incubation at 25°C for 10 min, absorbance was measured in triplicate at 562 nm with a microplate reader. EDTA (0–250 µg ml^{-1}) was used as the standard control. The results were expressed as milligrams of EDTA equivalents per gram of EO.

2.2.4 1,1-diphenyl-2-picrylhydrazyl radical scavenging activity assay

Free radical scavenging activity of DW_EO was quantified using previously described methodology (Touma et al., 2020). Briefly, 70 µL of 0.2 mM DPPH solution dissolved in methanol was mixed with 20 µL of EO or Trolox at concentrations of 0–1,000 µg ml^{-1}; the mixture was incubated at room temperature (22°C) and in the dark for 30 min and then absorbance was measured with a microplate reader. All analyses were performed in triplicate and the results were expressed as IC_{50} values in µg·ml^{-1} (defined as the concentration of EO required to inhibit 50% DPPH radicals present in the solution).

2.2.5 ABTS radical-scavenging activity assay

The ABTS radical scavenging activity of DW_EO was quantified following a previously described method (Touma et al., 2020). To prepare the working ABTS solution, 7 mM ABTS in PBS (pH 7.4) was mixed with 2.5 mM $K_2S_2O_8$ (final concentration), followed by storage in the dark at room temperature for 16 h. After radical generation, the mixture was diluted with PBS to an absorbance of 0.700 ± 0.02 units at 734 nm. Then, 20 µL of each diluted solution of EO or Trolox as the standard in the concentration range of 0–1,000 µg ml^{-1} was mixed with 180 µL of ABTS solution. Absorbance was measured 6 min after initial mixing at 734 nm with a microplate reader (BioTek Synergy HTX Multimodal Kit). All measurements were performed in triplicate. Scavenging activity was expressed as calculated IC_{50} values in µg·ml^{-1} (defined as the concentration of EO required to inhibit 50% ABTS radicals present in the solution). As blank, 180 µL solution of ABTS moiety in 20 µL of PBS was used.

2.3 Theoretical chemistry reactivity

2.3.1 Density functional theory calculations

DFT calculations for the five compounds from DW_EO including Kaurene, α-Eudesmol, γ-Eudesmol, Elemol and β-Caryophyllene selected for their antioxidant, antimicrobial, and antitumoral activity, were drawn using Discovery Studio (BIOVIA, Dassault Systèmes; Discovery Studio Modeling Environment 3.1. Dassault Systèmes: San Diego. 2017; Accelrys, CA). Geometries were optimized using Minnesota hybrid meta-GGA functional M08HX (Zhao and Truhlar, 2008) and the 6–31 + G(d,p) basis set (Del Bene et al., 1995), with Solvation Model Based on Density (SMD) for the implicit water. The M08HX functional can investigate the

intermolecular and intramolecular nonbonding interactions well (Zhao and Truhlar, 2008). All calculations were carried out using the Gaussian16 program (Frisch et al., 2016), to performed molecular electrostatic potential (MEP), firstly a calculation of their electron density and electrostatic potential was performed, using the cubegen tool of the Gaussian16 computational package (Frisch et al., 2016). Some DFT-based global and local reactivity descriptors, such as HOMO–LUMO gap, electronegativity (χ), global hardness (η), global electrophilicity index (ω), ionization potential (I), electron affinity (A), and Fukui functions, were calculated to better understand the reactivity of the molecules. The non-covalent interaction index (NCI) (Johnson et al., 2010; Contreras-García et al., 2011) was used to qualitatively identify the areas where weak interactions predominate, the origin of which may be dispersive in nature, hydrogen bonds, dipole-dipole interactions, or repulsive steric effects, which are based on the sign of the second eigenvalue (λ_2) of the electron density matrix (Hessian matrix) as is described in the literature (Sharma et al., 2018; Cantero-López et al., 2021). In this work, the promolecular densities (ρ^{pro}), computed as the sum of all atomic contributions, were used. The NCI was calculated using the NCIPLOT program (Contreras-García et al., 2011). The isosurfaces were visualised in Visual Molecular Dynamics (VMD) (Humphrey et al., 1996).

2.3.2 Molecular docking

Molecular docking analyses were performed to study the possible binding modes of Kaurene, α-Eudesmol, γ-Eudesmol, Elemol and β-Caryophyllene essential oils to IKBα/NF-κB (Huxford et al., 1998), Lipoxygenase (Borbulevych et al., 2004), CYP2C9 (Williams et al., 2003), NADPH-oxidase (Lountos et al., 2006) and Xanthine-oxidase (Cao et al., 2010) as potential inhibitors. AutoDock (v 4.2.1) and AutoDock Vina (v 1.0.2) (Trott et al., 2010) were used for all dockings in this study. The three-dimensional coordinates of all structures were optimized using MOPAC 2016(Stewart, 1990) software by PM6-D3H4 semi-empirical method (Stewart, 2007; Řezáč and Hobza, 2012). The ligand files were prepared using the AutoDockTools packagen (Sanner, 1999). The Mulliken partial atomic charges of each ligand were determined with PM6-D3H4 semi-empirical method; this approach introduces dispersion and hydrogen-bonded corrections to the PM6 method. The crystal structure of IKBα/NF-κB (PDB Code: 1IKN), Lipoxygenase (PDB Code: 1N8Q), CYP2C9 (PDB Code: 1OG5), NADPH-oxidase (PDB Code: 2CDU) and Xanthine-oxidase (PDB Code: 3NRZ), were downloaded from the Protein Data Bank (Berman et al., 2000). The IKBα/NF-κB, Lipoxygenase, CYP2C9, NADPH-oxidase and Xanthine-oxidase were treated with the Schrödinger's Protein Preparation Wizard (Madhavi Sastry et al., 2013); polar hydrogen atoms were added, nonpolar hydrogen atoms were merged, and charges were assigned. Docking was treated as rigid and carried out using the empirical free energy function and the Lamarckian Genetic Algorithm provided by AutoDock Vina (Morris et al., 1998). The grid map dimensions were 25 × 25 × 25 Å^3, making the binding pocket of IKBα/NF-κB the centre coordinates 33.41, 34.35 and 21.32. The binding pocket of Lipoxygenase was defined the centre coordinates 22.45, 1.29 and 20.36. The binding pocket of CYP2C9 was defined the centre coordinates −19.82, 86.68 and 38.27. The binding pocket of NADPH-oxidase was defined the centre coordinates 19.40, −6.12 and −0.68, and the binding pocket of Xanthine-oxidase was defined the centre coordinates 37.48, 19.30 and 18.15. All other parameters were set as the default defined by AutoDock Vina. Dockings were repeated 40 times with space search exhaustiveness set to 80. The best interaction binding energy (kcal·mol^{-1}) was selected for evaluation. Docking results 3D representations were used Discovery Studio 3.1 (Accelrys, CA) molecular graphics system and VMD (Humphrey et al., 1996).

2.3.3 Molecular reactivity analysis

Based on the frontier molecular orbital theory, Koopman's approximation can calculate several chemical descriptors. These descriptors are useful for predicting the reactivity of both atoms and molecular systems and are divided into two groups: global and local descriptors. The former are particularly useful for analyzing the reactivity of a molecule in its entirety, while the latter allow for the analysis of specific regions within a molecular species. Ionization energy (I) and electron affinity (A) are probably the most used descriptors, and these are complemented by the local descriptors electronegativity (χ), global hardness (η), and global electrophilicity index (ω).

2.4 Antibacterial activity

2.4.1 Chemical materials and antibiotics

The DENT® antibiotic cocktail (SR014E), selective for HP growth, was purchased from Oxoid, United States (contains 10 mg ml^{-1} vancomycin; 5 mg ml^{-1} cefsulodin, 5 mg ml^{-1} amphotericin B, and 5 mg ml^{-1} trimethoprim). Other stocks of antibiotics used, include ampicillin (100 mg ml^{-1}) and tetracycline (12.5 mg ml^{-1}), as well as sesquiterpenes, β-Caryophyllen, and γ-Eudesmol (99% pure), which were purchased from Sigma-Aldrich (Gabriel et al., 2017).

2.4.2 Microbial strains

The bacterial strains used for microbiological tests, including *Staphylococcus aureus* (15 clinical isolates and the reference strain ATCC 25923) and *Escherichia coli* (15 clinical isolates and the reference strain ATCC 25922), were obtained from the Microbiology Laboratory collection, Department of Medical Technology, Universidad Diego Portales. Moreover, 15 clinical isolates of *Candida albicans* and *Candida parapsilosis* (ATCC 22019), which is used as a reference strain in the trials of the

genus *Candida*, were kindly provided by Dr. Alvarez, Institute of Biomedical Sciences, Faculty of Medicine, Universidad de Chile. The strains were grown on Mueller Hinton Agar at 37°C.

From the collection of clinical isolates of the Microbial Pathogenesis Laboratory, Faculty of Medicine, Diego Portales University, Santiago, Chile, seven strains of *Helicobacter pylori* were obtained. The bacteria were cultured on 1.5% Brucella agar (from BD, United States), supplemented with 5%–7% horse blood and 1: 200-diluted DENT cocktail and incubated for 3–7 days under microaerophilic conditions (10% CO_2) and 95% humidity at 37°C (Ultee et al., 2002; CLSI, 2012).

2.4.3 Agar disk diffusion assay

The agar disk diffusion assay was used to analyze the antibacterial and antifungal activity of the DW_EO. Briefly, 6 mm sterile filter paper discs (Whatman No. 1) were saturated with 10 µL of filter sterilized EO. The impregnated discs were then placed on the surface of Mueller Hinton BD® solid agar medium. The medium plates were pre-inoculated with the corresponding microorganisms (standard inoculum of 1×10^8 CFU ml^{-1}, which is equivalent to 0.5 McFarland standard). The plates were incubated overnight at 37°C, and the diameter of the zone of inhibition (in mm) around each disk (diameter of the zone of inhibition plus diameter of the disk). Sensi-Disc™ was used as a positive control for gram-positive and gram-negative strains.

2.4.4 Microplate assay

To determine MIC, the microdilution method in 96-well plates was used according to the instructions approved by the Clinical and Laboratory Standards Institute (CLSI, 2012). DW_EO was added at 10-fold decreasing serial concentrations into Mueller Hinton BD® Broth in 96-well plates. To inoculate the microplates, fresh bacterial suspensions were used (equivalent to 1×10^8 bacteria·ml^{-1}), and the plates were incubated as previously described (CLSI, 2012).

DW_EO was solubilized in DMSO) at 2% (v/v) (does not affect bacterial growth) and added to the previously inoculated microplates and M-MTT (5 mg/ml). The plates were incubated as described above for 1 day. Absorbance was measured at 600 nm to calculate MIC, as described in the Clinical and Laboratory Standards Institute (CLSI, 2012) protocol. Bacterial control microplates without EO and without bacteria were used as controls. Data were compared with ANOVA using the GraphPad Prism 5 to identify significant differences between the studied groups (CLSI, 2012).

2.5 Cytotoxicity

2.5.1 Cell lines culture

The human epithelial mammary cell lines MCF10A (non-tumoral) and MCF7 (tumoral) and the human epithelial renal cell lines HK-2 (non-tumoral), 786-O and ACHN (tumoral) were obtained from American Type Culture Collection (ATCC, Rockville, MD). The cells were cultured in Dulbecco's Modified Eagle's F-12 Medium (DMEM-F12; Gibco, United States) supplemented with 10% fetal bovine serum (FBS; Gibco, United States) and maintained at 37°C in 5% of CO_2 atmosphere. When the cells reach the 80% of confluence, were replicated. The numbers of generations of the cell lines were about 5–10. *In vitro* assays were performed in triplicate of three independent experiments for each cell line.

2.5.2 Crystal Violet proliferation assay

To evaluate the dose-response at given concentrations and the time-course of DW_EO (24 and 48 h), the cells were detached with Tripsin-EDTA 0.5% (Gibco, United States) and 5×10^3 cells/well were seeded and incubated in a 96-well cell plate with DMEM-F12 supplemented with 10% FBS for 24 h. The supernatant was removed, and the cells were washed 1x with PBS 1X (Gibco, United States) and treated with DW_EO at known concentrations (64, 32, 16, 8, 4, or 2 µg/ml) of DW_EO dissolved in DMEM-F12 supplemented with 1% FBS. The vehicle was DMSO 1% in DMEM-F12 supplemented with 1% FBS as a control treatment, (the DW_EO is dissolved in DMSO 1%). After 24 or 48 h the supernatant was discarded, the cells were washed with PBS 1X and incubated with 100 µl of crystal violet (CV) solution (0.2% w/v in ethanol 10%) (Gibco, United States) for 20 min. Then the CV solution was removed and Na_2HPO_4 (0.1 M, pH 4.5, in ethanol 50:50 v/v) (SIGMA, United States) was added to elute the intra-cellular colorant. The absorbance of each sample was measured at 570 nm. The results are shown as percentage of colour intensity and normalized to cells grown in DMSO 1% as the control treatment.

2.5.3 MTT proliferation assay

To evaluate the dose-response at given concentrations of DW_EO, 5×10^3 cells/well were seeded and incubated in a 96-well cell plate with DMEM-F12 10% FBS for 24 h. The cells were treated with DW_EO extract at known concentrations (64, 32, 16 µg/ml) dissolved in culture medium (DMEM 1% FBS) or control medium (DMSO 1% in DMEM 1% FBS). After 24 or 48 h, the supernatant was discarded and MTT solution was added to each well, according to the manufacturer's recommendation. The cells were incubated in the dark at 37°C for 2 h. After, the MTT solution was removed, and 100 µl of DMSO was added. The absorbance of each sample was measured at 570 nm. Results are shown as percent color intensity and normalized to cells grown in 1% DMSO as control treatment.

2.5.4 Statistical analysis

Results were analyzed by ANOVA One way for independent data with Tukey's test post-hoc. A $p < 0.05$, which was considered as statistically significant.

2.6 Toxicity

2.6.1 Maintenance of *C. elegans* culture

For toxicity assays, the wild strain of *C. elegans*, N_2, was used. The N_2 strain was maintained on agar plates with nematode growth medium (NGM) in the presence of a layer of *Escherichia coli* OP50. These plates were incubated at 20°C for 3 days. Subsequently, gravid nematodes were collected and treated in the presence of a chlorine solution (0.45 N NaOH and 2% HOCl) to obtain eggs. To hatch the eggs and obtain synchronized adult nematodes, eggs were placed in plates with OP50 for 3 days. Finally, nematodes were collected in M9 saline solution (1.5 g KH_2PO_4, 3 g Na_2HPO_4, 2.5 g NaCl, 0.5 ml of 1 M $MgSO_4$, and distilled water to raise the final volume to 500 ml) (Brenner, 1974).

2.6.2 Test preparation

The DW_EO was prepared at concentrations of 0.39, 0.78, 1.56, 3.12, 6.25, 12.5, 25, and 50.0 mg mL^{-1} and added at a final volume of 100 µL to 96-well plates. Control tests were performed with 1% DMSO and M9 saline solution. *C. elegans* (10 adult nematodes·$well^{-1}$) was used in each assay. The plates were incubated at 20°C for 24 and 48 h. The experiments were performed in triplicate and repeated twice. To determine the survival rate, all nematodes were counted at 24 and 48 h. Individuals were considered alive if they presented any motility of the tail, head, or pharynx during 5 s of observation and were considered dead otherwise. Counts were obtained to determine the mortality rate (Skantar et al., 2005).

2.7 Composition

The chemical characterization of the DW_EO (leaves) was performed using GC–MS analysis on a Varian series 431 gas chromatograph (Agilent Technologies, Inc., Santa Clara, CA, United States) equipped with a DB-5ms fused silica capillary column (30 × 0.25 mm; film thickness, 0.25 µm) with split/no-split injection and coupled to a 220 series mass detector (Agilent Technologies, Inc.). The following conditions were set helium as the carrier gas at 1.5 ml min^{-1} in constant flow; injection volume: 0.8 µl, with 1:80 split ratio; injector temperature: 250°C; oven temperature: 50–260°C at 2°C min^{-1}. The electron impact ionization (EI+) was set at 70 eV, with the ion source temperature of 260°C. Mass spectra were recorded within a range of 40–300 atomic mass units. Terpenes in EO were identified based on retention index (RI) relative to a homologous series of n-alkanes (C5-C28; PolyScience, Niles, IL, United States) under the same experimental conditions. Standards (γ-Eudesmol, β-Caryophyllen and Elemol Sigma-Aldrich®) and standard isolates were co-injected as identification standards. To calculate the Kovats index or linear retention index, the programmed temperature formula is used. Compounds were identified using an MS library (NIST 05 and Wiley; NIST/EPA/NIH Mass Spectral Library with Search Program, NIST data version 11; software version 2.0 g), available online at http://www.nist.gov/srd/nist1a.cfm and comparison with previously reported MS data (Adams, 2007).

TABLE 1 Antioxidant activity of *Drimys winteri* essential oil.

Essential oils	IC_{50}FRAP[a]	IC_{50} DPPH[b]	IC_{50} ABTS[b]
D. winteri	166.8 ± 27.9	492.7 ± 11.1^{+++}	203.0 ± 12.8$^{***,+++}$
Trolox	—	11.7 ± 2.1	35.6 ± 1.5

[a]Expressed in mg Gallic acid equivalent/g essential oil.
[b]Expressed in µg/mL.
All values were expressed as Means ± SEM (n = 4).
***significantly different ($p < 0.5$ and $p < 0.01$).
+++significantly different respect to control ($p < 0.001$).

3 Results

3.1 Antioxidant activity

The antioxidant activity of DW_EO was evaluated using three complementary *in vitro* colorimeteric methods. The results obtained for antioxidant activity are observed in the Table 1 for DW_EO.The IC_{50} (DPPH and ABTS) were significantly higher than of the Trolox standard, which showed that it exhibits moderate antioxidant activity as a free radical scavenger in the both tests (IC_{50} 492.7 ± 11.1 and 203.0 ± 12.8 µg/ml, respectively), when compared to the positive control Trolox. (IC_{50} 11.7 ± 2.1 and 35.6 ± 1.5 µg/ml, respectively). The FRAP assay is a good indicator of the reducing potential of antioxidants against the oxidative consequences of reactive oxygen species. It was observed that the reducing capacity of DW_EO showed a good reducing potential with 166.8 ± 27.9 mg Gallic acid equivalent/g essential oil Table 1.

3.2 Theoretical chemistry reactivity

Table 2 presents the chemical reactivity descriptors for Kaurene, α-Eudesmol, γ-Eudesmol, Elemol and β-Caryophyllene using the Koopman's approach. For α-Eudesmol, γ-Eudesmol and β-Caryophyllene, the ionization energy was low, indicating that these species are better electron density donors. Meanwhile, for γ-Eudesmol, electron affinity was lower than for other compounds, indicating that these species would hardly accept more electrons. This was also reflected in their electronegativity values relative to the other compounds. Moreover, α-Eudesmol, γ-Eudesmol and β-Caryophyllene molecules showed lower hardness values than Kaurene and Elemol,

TABLE 2 Calculated HOMO and LUMO energies, electronegativity (χ), global hardness (η), global electrophilicity index (ω), ionization potential (I), and electron affinity (A) (in eV) of Kaurene, α-Eudesmol, γ-Eudesmol, Elemol and β-Caryophyllene.

Compound	E_{HOMO}	E_{LUMO}	ΔE	χ	η	ω	I	A
Kaurene	−8.105	−0.278	7.827	4.192	3.914	2.245	8.105	0.278
α-Eudesmol	−7.701	−0.246	7.455	3.973	3.728	2.118	7.701	0.246
γ-Eudesmol	−7.590	−0.197	7.394	3.894	3.697	2.050	7.590	0.197
Elemol	−8.096	−0.286	7.810	4.191	3.905	2.249	8.096	0.286
β-Caryophyllene	−7.435	−0.252	7.183	3.843	3.592	2.056	7.435	0.252

indicating that they are less averse to electron arrival and are thus more reactive systems. For the highest occupied molecular orbital (HOMO) and the lowest unoccupied molecular orbitals (LUMO) energies and their difference. The order of energy gap was as follows: β-Caryophyllene < γ-Eudesmol < α-Eudesmol < Elemol < Kaurene. As the energy gap decreases, the reactivity of the molecule increases, and it can be easily excited by low energy. Remarkably, γ-Eudesmol and α-Eudesmol have hydroxyl groups that enable them to function as chelating agents. Meanwhile, with a lower energy gap, β-Caryophyllene, γ-Eudesmol and α-Eudesmol would be less favorable to reduction processes. Note, the energy gaps of β-Caryophyllene and γ-Eudesmol were smaller than other compounds; thus, β-Caryophyllene and γ-Eudesmol would be more reactive than compounds.

To simultaneously present electrophilic and/or nucleophilic activation at different sites of molecules, the Koopman's approach, which is based on the molecular border orbital theory, calculates global (as mentioned above) and local reactivity indices. For this type of analysis, the Fukui functions are used. In addition to their use for predicting reactive sites for nucleophilic (f^+) and electrophilic (f^-) attacks, these functions can be interpreted as the sensitivity measure of the chemical potential of a system to change in the external potential or a measure of how electron density varies as the number of electrons in the system increases. In the case of the sites identified for nucleophilic attack, all molecules, atoms present in parts of aromatic rings and alkyl groups were identified. α-Eudesmol, γ-Eudesmol and Elemol present a hydroxyl group as part of the reactive sites. In all molecules, atoms present in parts of aromatic rings and alkyl group were identified as sites for electrophilic attack. Considering the potential application of the tested molecules as antioxidants, it is interesting to elucidate the active sites. The α-Eudesmol, γ-Eudesmol and Elemol molecules present a hydroxyl group as part of the reactive site. These results are consistent with previous reports that α-Eudesmol and γ-Eudesmol act as an antioxidant (Dib et al., 2017). The Molecular Electrostatic Potential maps, Figure 1, the positive regions (blue/green) indicate the portion of the molecule most likely to undergo nucleophilic attack, while the negative regions (green/red) indicate regions most likely to undergo electrophilic attack. EPMs of α-Eudesmol, γ-Eudesmol and Elemol molecules showed negative zones (red) of electrostatic potential in the position of the hydroxyl groups, which are favored for electrophilic attacks. In EPMs of α-Eudesmol and γ-Eudesmol, aromatic rings present a slight negative zone, which can facilitate π–π stacking interactions. Thus, the attacking electrophile would be attracted to the negatively charged sites. These differences in the potential and charges around compounds may primarily be responsible for variations in their antioxidant activity.

3.3 Molecular docking analysis

According to the obtained results in Figure 2. The molecular docking experiments showed more favorable interactions with CYP2C9 target, with an average binding energy −7.7 kcal mol^{-1}, as compared to IKBα/NF-κB, Lipoxygenase, NADPH-oxidase, and Xanthine-oxidase targets, which have an average binding energy of −6.8, 1.4, −7.34 and −7.04 kcal mol^{-1}.

To describe the binding and interaction of the ligands with CYP2C9, the AutoDock Vina tool was used to explore how the ligand binds to the respective protein. The best structural information was considered for the analyses shown in Figure 2 and Table 3. Figure 3 shows the functionally interacting residues and the mode of ligand binding to the CYP2C9 site. The molecular docking results, revealed the involvement of the Leu366, Ile99, Phe114, Ala103 and Val113 residues, favoring the essential oils binding, as they present auspicious alkyl-aromatic binding interactions with the essential oils. These interactions form a nonpolar-hydrophobic pocket that contributes to the binding of these compounds. Mutational screening of these residues could be very effective in subsequent studies. Several types of interactions observed between essential oils and CYP2C9, such as π-alkyl, hydrophobic and hydrophilic interactions, hydrogen bonds and Van der Waal interactions, in addition to steric interactions, determine the binding of essential oils to CYP2C9. The binding modes of Kaurene, α-Eudesmol, γ-

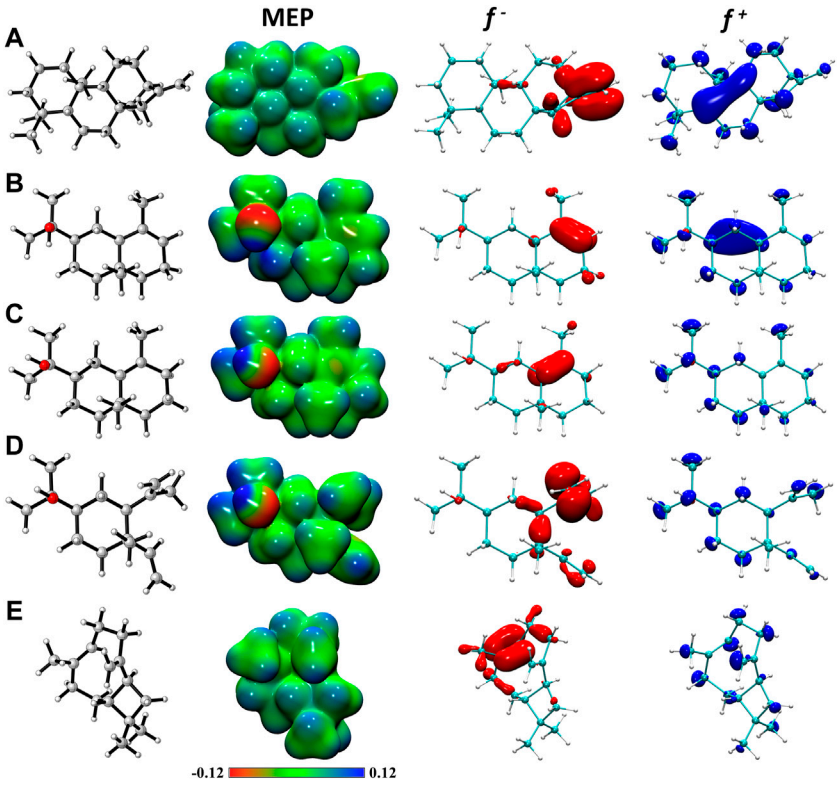

FIGURE 1
Molecular electrostatic potential maps (in a.u.) and graphical representation of the electrophilic f^- and nucleophilic f^+ Fukui functions of **(A)** Kaurene, **(B)** α-Eudesmol, **(C)** γ-Eudesmol, **(D)** Elemol and **(E)** β-Caryophyllene. All isosurfaces for Fukui functions were generated at a 0.0025 a.u. at the M08HX/6-31+G (d, p) level of theory.

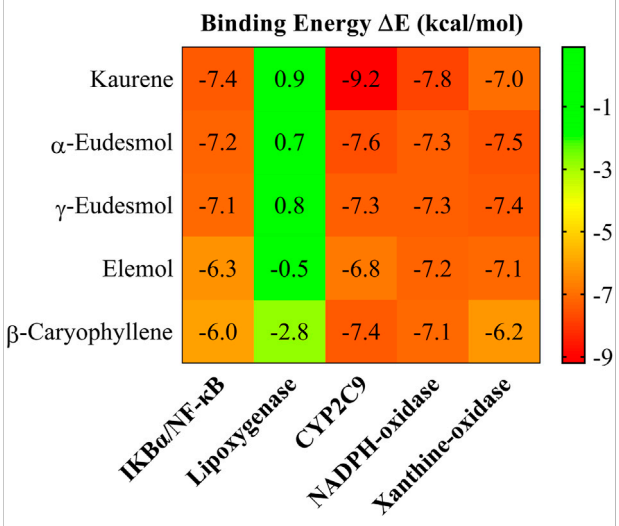

FIGURE 2
Heat map of the intermolecular docking energy values (kcal·mol^{-1}) of the Kaurene, α-Eudesmol, γ-Eudesmol, Elemol and β-Caryophyllene essential oils.

Eudesmol, Elemol, and β-Caryophyllene to the CYP2C9 binding site are shown in Figure 2. For Kaurene at the CYP2C9 binding site, it shows π-alkyl aromatic and Van der Waals type interactions, where it forms interactions with Phe114, Leu366, Pro367, Ile213, Ile99 and Ala103 residues. In the case of α-Eudesmol and γ-Eudesmol, they present a hydrogen bond interaction between the hydroxyl group with Arg433 and Cys435 on backbone protein; π-alkyl aromatic and Van der Waals with Trp120, Ala297, Leu366, Ile112, Val113 and Val436 residues. For Elemol, it shows π-alkyl aromatic and Van der Waals type interactions, where it forms interactions with Phe100, Phe114, Phe476, Ala103, Ile99, Val113 and Leu366 residues. In the case of β-Caryophyllene, they present similar π-alkyl aromatic and Van der Waals interactions with Phe100, Phe114, Leu102, Ala103, Leu366, and Pro307 residues. All these interactions between the five essential oils and the CYP2C9 binding site are shown in Figure 2 in detail in the isosurfaces of the non-covalent interactions, where π-alkyl aromatic and Van der Waals type interactions are mostly observed, due to their green-coloured isosurfaces.

TABLE 3 Active pockets on the essential oils in the CYP2C9.

	Interacting amino acids in the binding pocket
Compound	**CYP2C9**
Kaurene	Leu366, Pro367, Ile213, Ile99, Phe114, Arg97, Ala103
α-Eudesmol	Ala297, Leu366, Ser429, Arg433, Trp120, Ile112, Val113, Val436, Cys435
γ-Eudesmol	Ala297, Val113, Leu366, Cys435, Arg433, Trp120, Ile112, Val436
Elemol	Phe100, Ala103, Ile99, Arg97, Phe114, Val113, Leu366, Phe476
β-Caryophyllene	Phe100, Leu102, Ala103, Phe114, Leu366, Pro307

3.4 Antimicrobial activity

Results obtained for antimicrobial activity for DW_EO are observed in Table 4, in general the essential oil obtained from *D. winteri* leaves has effect against *H. pylori* (MIC 32 μg/ml), *S. aureus* (MIC 8 μg/ml), *E. coli* (MIC 32 μg/ml) and *C. albicans* (MIC 64 μg/ml), thus a greater effect of the essence against *S. aureus*, even if it is compared with the effect, its major compounds β-Caryophyllen and γ-Eudesmol (MIC 64 μg/ml).

3.5 Cytotoxicity

The DW_EO presents selective inhibitory activity on epithelial tumor cells. To assess the selective cytotoxicity and the antitumoral activity of the DW_EO, mammary tumor cell line, MCF-7 was incubated with DW_EO at different concentrations and a MTT assay was conducted. The findings show that the MCF-7 epithelial cells displayed an inhibited proliferation when treated with DW_EO at different concentrations (64 to 16 μg/mL). It was found that at lower concentrations (8 μg/mL) it did not show any effects (Figure 4). Due to this result, the mammary tumor cell line MCF-7 and the mammary non-tumor cell line MCF10A, were incubated with DW_EO at two different concentrations (64 μg/ml and 32 μg/ml), and a proliferation CV assay was performed. DW_EO significantly inhibited the proliferation of mammary tumor MCF-7 cells (Figure 5A). Conversely, in the MCF10A non-tumoral cells no significant differences were found among the treatments (Figure 5B). The human epithelial renal cells (HK-2, 786-O and ACHN) were exposed to the DW_EO and a dose-response curve was performed (64 μg/ml and 32 μg/ml). In contrast to the effect observed in non-tumoral mammary cells, the DW_EO showed an inhibitory effect on proliferation of non-tumor renal cell HK-2 (Figure 6A). Regarding the primary tumor (786-O) and metastatic site (ACHN) renal cell lines, the DW_EO treatment demonstrated a significant inhibition on cell viability and proliferation (Figures 6B,C respectively).

3.6 Toxicity

DW_EO showed low or no toxicity against *C. elegans* (Figure 7). Although some level of toxicity was observed, it was only at the highest 25–50 mg/ml, the same was observed at 24 h (Figure 7A) and 48 h (Figure 7B) of study. It is observed a decrease in survival to the EO concentration of 50 mg/ml , showed low toxicity and dose dependent.

3.7 Composition

The results show the essential oil of *D. winteri* characterized by CG-MS analysis in Table 5 and Figure 8, had a total of 5 main compounds identified, 4 sesquiterpenes (β -Caryophyllen, Elemol, γ-Eudesmol, α-Eudesmol) and 1 diterpene (Kaurene) were determined. Among them the most abundant γ -Eudesmol in 39.7%, β -Caryophyllen in 33.7% and Elemol 25.9%, the less abundant Kaurene in 0.4% and α- Eudesmol in 0.3%.

4 Discussion

The results described for the antioxidant activity of DW_EO, show a moderate activity of the oil components to donate or transfer hydrogen atoms, that is, as free radical scavengers (Huang et al., 2005; Moon and Shibamoto, 2009). The DPPH test allows evaluating the activity in organic media (especially alcoholic media), while the ABTS test allows to assess the antioxidant activity of hydrophilic and lipophilic compounds at physiological pH (Table 1) (Moon and Shibamoto, 2009). It is important to note that this is the first time that the antioxidant activity of DW_EO has been studied. The antioxidant activity of hydroxylated compounds such as γ-Eudesmol and α-Eudesmol, which are found in the essence at 39.7 and 0.3% respectively, has been previously described (Miguel, 2010; Goodarzi et al., 2016). The FRAP assay was used to determine the reducing power of DW_EO and the relationship between its antioxidant effect and

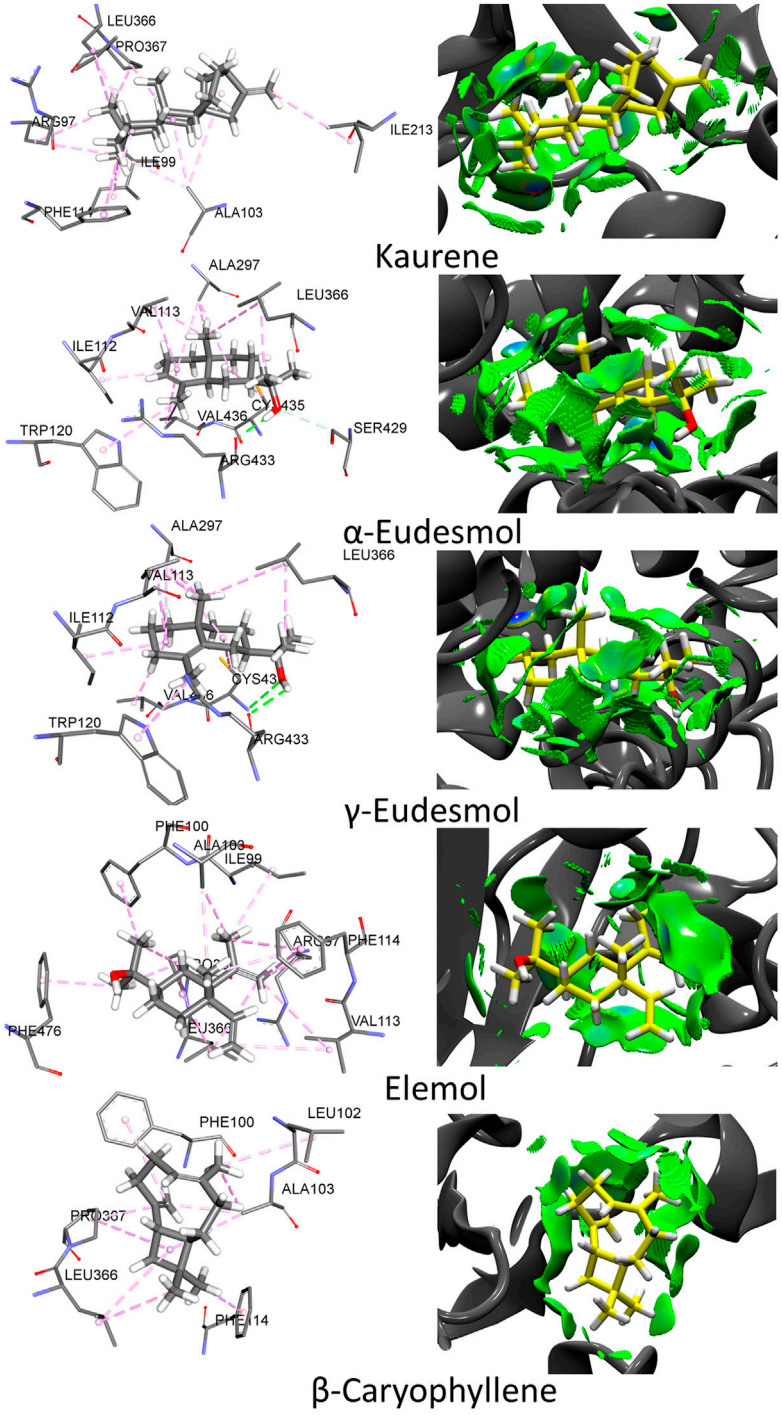

FIGURE 3
Molecular docking and no-covalent interactions for the Kaurene, α-Eudesmol, γ-Eudesmol, Elemol and β-Caryophyllene essential oils bound to CYP2C9. The surrounding amino acid residues in the binding pocket of CYP2C9 within 3.5 Å. The isosurfaces are colored according to the signed λ_2 value using a Blue-Green-Red (BGR) color scale: red (repulsive region), green (weak interactions), and blue (strong attractive interactions).

its reducing effect potential. As shown in different assay, the DW_EO exhibited ability. This result is in agreement with the findings of the ABTS and DPPH assay and confirms that the antioxidant DW_EO power may be due to electron transfer mechanisms. Although no aromatic phenolic compounds were identified in oil, there are reports of other AEs that in the absence

TABLE 4 The MIC_{50} values of DW_EO and their major components using M-MTT against clinical isolates of *H. pylori, S. aureus, E. coli,* and *C. albicans*.

EO or its purified component	MIC (μg/ml) *H. pylori*	MIC (μg/ml) *S. aureus*	MIC (μg/ml) *E. coli*	MIC (μg/ml) *C. albicans*
DW_EO	32	8	32	64
β-Caryophyllen	64	64	64	64
γ-Eudesmol	64	64	64	64

The ANOVA analysis including the Tukey test did not show significant differences between the β-caryophyllen and γ-eudesmol purified compounds. The values were an average of 7 isolates for *H. pylori* and 15 isolates for the other species and the whole experiment was done in triplicate.

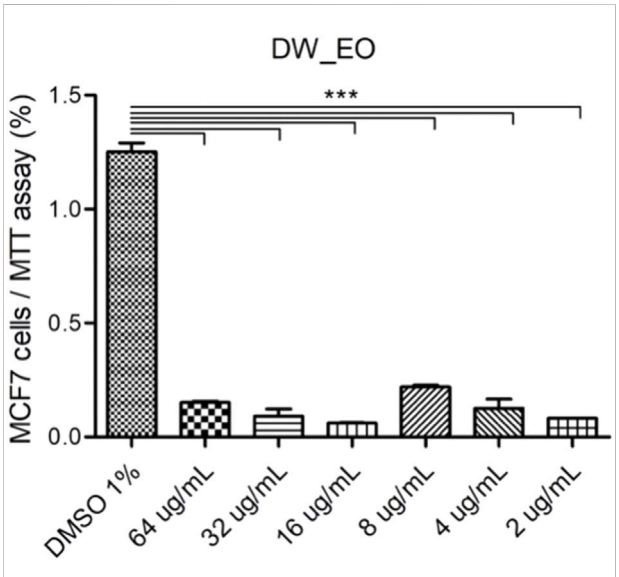

FIGURE 4
Dose-response curve of human epithelial mammary tumor cell line MCF-7 treated with DW_EO. The graph bar corresponds to the proliferation of MCF7 treated with the EO at different concentrations, versus control (DMSO 1%) for 48 h, evaluated by CV assay at 570 nm. Three independent experiments, in triplicate, were performed for each treatment and concentration. *** $p < 0.001$.

of this type of compounds, have presented a high antioxidant capacity comparable to the synthetic antioxidant BHT (Miguel, 2010; Goodarzi et al., 2016) In addition, interestingly, some hydroxyl groups of γ-Eudesmol and α-Eudesmol could act as chelating agents, reducing the production of radical species by Fe^{+2}.

It is important to consider that the DW_EO antioxidant activity is the result of the individual activity of each component, since these can react with radical species or inhibit their generation. Thus, a component present in low proportion in the mixture could have a high antioxidant capacity that is not reflected in the mixture. To evaluate the contribution of each component of the DW_EO, computational studies were performed to estimate the individual antioxidant capacity and the possibility of acting on the enzymatic generation of free radicals (Rajan and Muraleedharan, 2017). In addition, reactivity indices of each component were calculated to explain their possible role in antimicrobial activity.

Based on the MEP, it is proposed that the hydroxyls of α-Eudesmol, γ-Eudesmol and Elemol favor electrophilic attacks and that the aromatic rings present in α-Eudesmol and γ-Eudesmol, facilitate π-π stacking interactions, thus enhancing their reactivity. These results suggest an antioxidant capacity based on their chemical reactivity. Considering that they show a smaller energy gap, it could be less favorable to the reduction

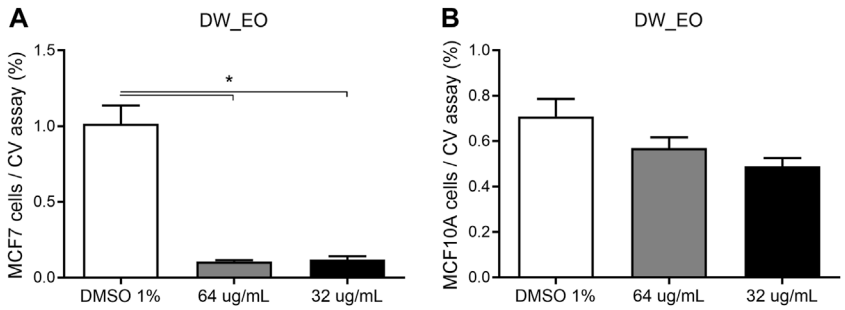

FIGURE 5
Dose-response curve of human epithelial mammary tumor cell line MCF-7 **(A)** and non-tumor cell line MCF10A **(B)** treated with DW_EO. The graph bar corresponds to the proliferation of MCF7 and MCF10A treated with EOs at different concentrations versus control (DMSO 1%) for 48 h, evaluated by CV assay at 570 nm. Three independent experiments, in triplicate, were performed for each treatment and concentration. *** $p < 0.001$.

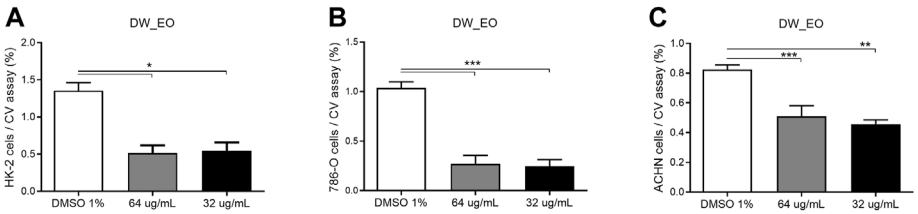

FIGURE 6
Dose-response curve of human epithelial renal non-tumor cell line HK-2 **(A)**, and tumor cell lines 786-0 **(B)** and ACHN **(C)** treated with DW_EO. The graph bar corresponds to the proliferation of HK-2, 786-O and ACHN treated with DW EO at different concentrations versus control (DMSO 1%) for 48 h, evaluated by CV assay at 570 nm. Three independent experiments, in triplicate, were performed for each treatment and concentration. *** $p < 0.001$.

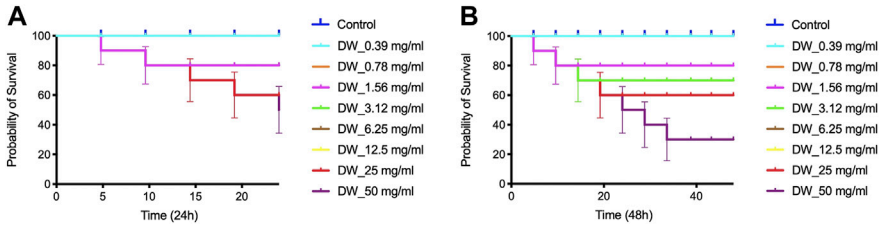

FIGURE 7
(A) Percent survival DW (*D. winteri*) essential oils against *C. elegans* 24 h **(B)** Percent survival DW (*D. winteri*) essential oils against *C. elegans* 48 h.

TABLE 5 Compounds from GC-MS analyses of DW_EO and the respective calculated Kovats index (KI cal) and from the literature (KI lit).

Fraction number	Retention time (min)	CAS	KI cal	KI lit	%	Name
1	23.7	87-44-5	—	1418	**33.7**	**β -Caryophyllen***
2	26.9	639-99-6	1562	1547	**25.9**	**Elemol***
3	28.9	1209-71-8	1580	1627	**39.7**	**γ-Eudesmol***
4	29.4	473-16-5	1506	1652	0.3	α-Eudesmol*
5	37.5	562-28-7	—	2043	0.4	Kaurene**

Sesquiterpenes*.
Diterpenes**.
Approximate retention times.

processes on β-Caryophyllene, the γ-Eudesmol and the α-Eudesmol (Hossen et al., 2021). This antioxidant capacity, for the case of γ-Eudesmol and α-Eudesmol, may be favored to act as chelating agents for metals such as Fe^{+2}. Furthermore, the studied compounds show favorable binding energy with the targets IKBα/NF-κB, NADPH-oxidase and Xanthine oxidase, however the highest binding energy was with CYP2C9, highlighting its affinity for Keurene. Due to its high activity, CYP2C9 is one of the enzymes responsible to produce oxygen-derived free radicals. Thus, these results suggest that the studied compounds could act as antioxidants, it may also indicate interaction with these enzymes.

The results obtained for antimicrobial activity for DW_EO, show a greater effect on gram-positive bacteria compared to gram-negative bacteria and yeast, highlighted *S. aureus* (MIC 8 μg/ml), even if it is compare with the effect its major components β-Caryophyllen and γ -Eudesmol (MIC 64 μg/ml). There are no studies of the DW_EO in the strains, however, the antifungal activity of front phytopathogenic fungi and insecticidal properties has been described (Muñoz et al., 2021).

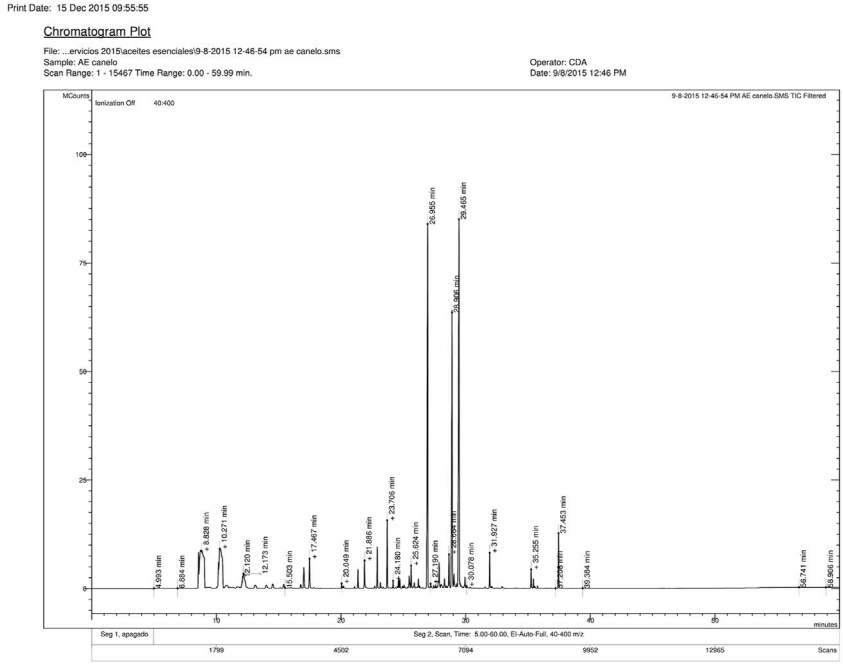

FIGURE 8
Chromatographic GC profile of *Drimys winteri* essential oil.

Essential oils (EOs) offer a plethora of bioactivities including antioxidant, anti-mutagenic, and antiproliferative properties. The antiproliferative activity is related with apoptosis, necrosis, arrest of cell cycle, and dysfunctioning of main cell organelles (Sharifi-Rad et al., 2017).

It has been reported that the EOs can inhibit the tumor cells proliferation and viability at low concentrations, meanwhile epithelial non-tumor cells are not affected (Sharma et al., 2022). Results show that DW_EO exerts an inhibitory effect on proliferation and viability in human tumor epithelial cell lines from mama and kidney (MDA-MB-231 and MCF7; ACHN and Casi-1 respectively). These results are consistent with those of various authors, who report similar EOs effects of the same plant species (Montenegro et al., 2014; Russo et al., 2019) and other members of the Winteraceae family (Allouche et al., 2009). The selective cytotoxic effect of DW_EO did not affect human non-tumoral epithelial cell lines MCF10A (mammary) and HK-2 (renal), that present normal proliferative activity. Regarding the proliferation and viability of these cells, it is observed that the EOs, suggesting a selective cytotoxic effect that can be related with the low metabolic activity of these cells compare to human tumoral cell lines with a metabolic activity increased, did not affect them.

The results obtained for the toxicity for DW_EO showed low toxicity against *C. elegans*, similar to those recommended in *C. elegans* studies (1 mg/ml) (Dal Forno et al., 2019). Satyal and Dosoky, reported marginally EO toxicity obtained from *Amomum subulatum* (Satyal et al., 2012). Similar results were reported by Larrazabal-Fuentes using essential oils from *Rica Rica* and *Copa Copa* against *C. elegans* (Larrazabal-Fuentes et al., 2019). Likewise, Touma and collaborators reported that essential oils of Peumo (*Cryptocarya alba*) and Laurel (*Laurelia sempervirens*) showed toxicity in higher concentrations than 12.5 mg/ml, demonstrating that essential oils of herbs presented low or null toxicity (Touma et al., 2020). With respect to the terpenes presented in the essence, some researchers have reported insecticidal activity. Nararak et al. determined that β-Caryophyllene oxide could be considered as a safe and effective repellent against mosquitoes (Nararak et al., 2020). Anaya and collaborators attribute to caryophyllene present on orange oil (*Citrus sinensis* L.) has an effect on larvicidal activity (Anaya-Gil et al., 2021).

Balasubramani and collaborators studied the larvicidal and repellent activity of *Artemisia vulgaris* leaf essential oil against the dengue vector *Aedes aegypti* (Balasubramani et al., 2018) and biosynthesized gold nanoparticles integrated ointment base for repellent activity against *Aedes aegypti* L. (Sundararajan et al., 2022). Balasubramani et al. developed nanoemulsions from essential oil of *Vitex negundo* L. and demonstrated their antioxidant, antimicrobial and larvicidal efficacy (*Aedes aegypti* L.) (Balasubramani et al., 2017; Balasubramani et al., 2021).

The low toxicity results obtained with EO_DW against *C. elegans* allow future *in vivo* studies to be planned to try to

determine the mechanisms of action of this essence in the different biological activities studied, or to develop a nanoemulsion type formulation with biopesticide activity (Balasubramani et al., 2018).

Results exhibit three mayor sesquiterpenes γ-Eudesmol in 39.7%, β -Caryophyllen in 33.7% and Elemol in 25.9% (Table 5). Other studies, such as Barrero and Herrador, identified two components in high abundance, α-pinene (14.9%) and α-cubebene (10.9%) (Barrero et al., 2000). Monzávez et al. described that the oil components found in greater concentration were α-pinene (60.78%), β-pinene (12.09%), limonene (2.70%), and β-myrcene (2.50%) (Monsálvez et al., 2010). Muñoz and Christen found α-pinene (23.1%) β-pinene (43.6%) and linalool (10.5%) of Island plants with as the main components in the leaves, while sesquiterpenes (germacrene D 17.6%) and phenylpropanoids (safrole 20.8%) (Muñoz et al., 2011). Tampe and Espinoza found the oxygenated sesquiterpenes elemol (13.5%), γ-eudesmol (11.4%), β-eudesmol (8.4%) and α-eudesmol (6.3%) and the monoterpene hydrocarbons α-pinene (7.9%) and β-pinene (5.1%) were the most abundant compounds in the EO of *D. winteri* (Tampe et al., 2020). Only α-eudesmol was observed in common with the investigation (Tampe et al., 2020). The leaves of *D. winteri* J.R. et G. Forst were collected, in September 2015 from Curiñanco (39°48′30″ S and 73°14′30″ W) Valdivia, Chile, unlike Barrero and Heerrador (Barrero et al., 2000), which sample was collected in September 1992 in Villarrica (Chile). Monzálvez and collaborators collected bark from an adult *D. winteri* trees in January of 2007, in the town of San Ignacio, Ñuble Province, Chile (36°51′S, 71°57′W) (Monsálvez et al., 2010). Tampe and Espinoza obtained leaves and twigs of *D. winteri* in mid-October 2008 on a farm located at 38°58'S, 72°48′W, near Freire, in the central plain of the Araucanía Region; perhaps this would explain the difference in the observed chemotypes. Although the majority of the compounds found in this work coincide with those reported by some authors, the relative abundances vary in the essences, which could be explained by differences in geographical location, humidity, exposure to the Sun, and bioclimatic conditions. (Ben Abada et al., 2020; Tampe et al., 2020).

In summary, this study demonstrated that essential oil obtained from *D. winteri* leaves, has antioxidant activity *in vitro*, antibacterial activity on gram-positive bacteria, selective antiproliferative activity against tumor cell lines and low toxicity against *C. elegans*. This work provides new information such as antimicrobial and antioxidant activity, complements the antiproliferative activity previously described only for human melanoma, including studies in tumor and normal mammary and renal cells, and the toxicity against *C. elegans* was studied. It is important to continue studying the mechanisms and to carry out *in vivo* studies that allow the projection of biomedical applications of this essential oil.

Data availability statement

The original contributions presented in the study are included in the article/Supplementary Material, further inquiries can be directed to the corresponding author.

Author contributions

Conceptualization: JB and ML-F; methodology: KF, MN, JT, AP, IN, and FB; investigation: FU, JT, MN, BS, AP, KF, ML-F, IN, MF, FB, MO, OY, and JB; writing—original draft preparation: JB, AP, MO, FB, and ML-F; writing—review and editing and funding acquisition: AP, IN, MF, FB, MO, OY, and JB. All authors have read and agreed to the published version of the manuscript.

Funding

This work was supported by Universidad Diego Portales (Proyecto Semilla 201521) and (Proyecto Académicas 1130327006).

Acknowledgments

Eduardo Álvarez, Instituto de Ciencias Biomédicas, Facultad de Medicina, Universidad de Chile. Pedro Cortes TM, Facultad de Salud y Odontología, Universidad Diego Portales. Gino Corsini of the Universidad Automona de Chile. To our dear colleague and friend Alejandro Venegas (1945–2021), whom was an important part of this work and taught us to work with *Helicobacter pylori* among other things.

Conflict of interest

The authors declare that the research was conducted in the absence of any commercial or financial relationships that could be construed as a potential conflict of interest.

Publisher's note

References

Adams, R. (2007). *Identification of essential oil components by gas chromatography/quadrupole mass spectroscopy*. 4th Edition. *Carol. Stream*: Allured Publishing Corporation, 65–120.

Allouche, N., Apel, C., Martin, M. T., Dumontet, V., Guéritte, F., and Litaudon, M. (2009). Cytotoxic sesquiterpenoids from Winteraceae of caledonian rainforest. *Phytochemistry* 70, 546–553. doi:10.1016/j.phytochem.2009.01.012

Anaya-Gil, J., Cabarcas-Caro, A., Leyva-Ricardo, M., Parra-Garrido, J., Gaitan-Ibarra, R., and Vivas-Reyes, R. (2021). Artificial modification of the chemical composition of orange oil (Citrus sinensis L.) and its effect on larvicidal activity. *Saudi J. Biol. Sci.* 28, 1913–1918. doi:10.1016/j.sjbs.2020.12.042

Avello Lorca, M., López Canales, C., Gatica Valenzuela, C., Bustos Concha, E., Brieva Chait, A., Pastene Navarrete, E., et al. (2012). Efectos antimicrobianos de extractos de plantas chilenas de las familias Lauraceae y Atherospermataceae. *Rev. Cubana Plantas Med.* 17, 73–83.

Balasubramani, S., Rajendhiran, T., Moola, A. K., and Diana, R. K. B. (2017). Development of nanoemulsion from Vitex negundo L. essential oil and their efficacy of antioxidant, antimicrobial and larvicidal activities (*Aedes aegypti* L.). *Environ. Sci. Pollut. Res.* 24, 15125–15133. doi:10.1007/s11356-017-9118-y

Balasubramani, S., Ranjitha Kumari, B. D., Moola, A. K., Sathish, D., Prem Kumar, G., Srimurali, S., et al. (2021). Enhanced production of β-caryophyllene by farnesyl diphosphate precursor-treated callus and hairy root cultures of Artemisia vulgaris L. *Front. Plant Sci.* 12, 634178. doi:10.3389/fpls.2021.634178

Balasubramani, S., Sabapathi, G., Moola, A. K., Solomon, R. V., Venuvanalingam, P., and Bollipo Diana, R. K. (2018). Evaluation of the leaf essential oil from Artemisia vulgaris and its larvicidal and repellent activity against dengue fever vector Aedes aegypti—an experimental and molecular docking investigation. *ACS Omega* 3, 15657–15665. doi:10.1021/acsomega.8b01597

Barrero, A., Herrador, M., Arteaga, P., Lara, A., and Cortés, M. (2000). Chemical composition of the essential oil from drimys winteri forst. Wood. *J. Essent. Oil Res.* 12, 685–688. doi:10.1080/10412905.2000.9712190

Ben Abada, M., Haouel Hamdi, S., Masseoud, C., Jroud, H., Bousshih, E., and Mediouni Ben Jemâa, J. (2020). Variations in chemotypes patterns of Tunisian Rosmarinus officinalis essential oils and applications for controlling the date moth Ectomyelois ceratoniae (Pyralidae). *South Afr. J. Bot.* 128, 18–27. doi:10.1016/j.sajb.2019.10.010

Berman, H. M., Westbrook, J., Feng, Z., Gilliland, G., Bhat, T. N., Weissig, H., et al. (2000). The protein Data Bank. *Nucleic Acids Res.* 28, 235–242. doi:10.1093/nar/28.1.235

Borbulevych, O. Y., Jankun, J., Selman, S. H., and Skrzypczak-Jankun, E. (2004). Lipoxygenase interactions with natural flavonoid, quercetin, reveal a complex with protocatechuic acid in its X-ray structure at 2.1 Å resolution. *Proteins.* 54, 13–19. doi:10.1002/prot.10579

Brenner, S. (1974). The genetics of *Caenorhabditis elegans*. *Genetics* 77, 71–94. doi:10.1093/genetics/77.1.71

Burgos, V., Paz, C., Saavedra, K., Saavedra, N., Foglio, M. A., and Salazar, L. A. (2020). Drimenol, isodrimeninol and polygodial isolated from Drimys winteri reduce monocyte adhesion to stimulated human endothelial cells. *Food Chem. Toxicol.* 146, 111775. doi:10.1016/j.fct.2020.111775

Cantero-López, P., Robledo Restrepo, S. M., Yañez, O., Zúñiga, C., and Santafé-Patiño, G. G. (2021). Theoretical study of new LmDHODH and LmTXNPx complexes: Structure-based relationships. *Struct. Chem.* 32, 167–177. doi:10.1007/s11224-020-01624-7

Cao, H., Pauff, J. M., and Hille, R. (2010). Substrate orientation and catalytic specificity in the action of xanthine oxidase: The sequential hydroxylation of hypoxanthine to uric acid. *J. Biol. Chem.* 285, 28044–28053. doi:10.1074/jbc.m110.128561

CLSI (2012). "Performance standards for antimicrobial disk susceptibility tests, approved standard," in *CLSI document M02-A11, 950 west valley road, suite 2500*. Editor C. A. L. S. Institute (Wayne, Pennsylvania 19087, USA.: Cochin Academy for Language Studies).

Contreras-García, J., Johnson, E. R., Keinan, S., Chaudret, R., Piquemal, J.-P., Beratan, D. N., et al. (2011). NCIPLOT: A program for plotting noncovalent interaction regions. *J. Chem. Theory Comput.* 7, 625–632. doi:10.1021/ct100641a

Dal Forno, A. H., Câmara, D., Parise, B., Rodrigues, C. F., Soares, J. J., Wagner, R., et al. (2019). Antioxidant and lipid lowering effects of dried fruits oil extract of Pterodon emarginatusin *Caenorhabditis elegans*. *Arabian J. Chem.* 12, 4131–4141. doi:10.1016/j.arabjc.2016.04.001

Del Bene, J. E., Person, W. B., and Szczepaniak, K. (1995). Properties of hydrogen-bonded complexes obtained from the B3LYP functional with 6-31G(d,p) and 6-31+G(d,p) basis sets: Comparison with MP2/6-31+G(d,p) results and experimental data. *J. Phys. Chem.* 99, 10705–10707. doi:10.1021/j100027a005

Dib, I., Fauconnier, M.-L., Sindic, M., Belmekki, F., Assaidi, A., Berrabah, M., et al. (2017). Chemical composition, vasorelaxant, antioxidant and antiplatelet effects of essential oil of Artemisia campestris L. from Oriental Morocco. *BMC Complement. Altern. Med.* 17, 82. doi:10.1186/s12906-017-1598-2

Fratoni, E., de Athayde, A. E., da Silva Machado, M., Zermiani, T., Venturi, I., Corrêa Dos Santos, M., et al. (2018). Antiproliferative and toxicological properties of drimanes obtained from Drimys brasiliensis stem barks. *Biomed. Pharmacother.* 103, 1498–1506. doi:10.1016/j.biopha.2018.04.103

Frisch, M. J., Trucks, G. W., Schlegel, H. B., Scuseria, G. E., Robb, M. A., Cheeseman, J. R., et al. (2016). *Gaussian 16 rev. C.01*. Wallingford, CT: Carnegie Mellon University Gaussian, Inc.

Gabriel, B., Gonzalo, S., Susana, F., Inés, F., Urbina, A., and Rodríguez, J. C. (2017). Repelencia de Mezclas de Aceites Esenciales de Boldo, Laurel Chileno, y Tepa Contra el Gorgojo del Maíz. *Southwest. Entomol.* 42, 551–562. doi:10.3958/059.042.0224

Goodarzi, S., Hadjiakhoondi, A., Yassa, N., Khanavi, M., and Tofighi, Z. (2016). Essential oils chemical composition, antioxidant activities and total phenols of Astrodaucus persicus. *Iran. J. Basic Med. Sci.* 19, 159–165.

Hernández, V., Becerra, J., Becerra, J., Bittner, M., Silva, M., and Brintrup, C. (2010). Actividad de aceites esenciales de Canelo, Queule, Bailahuén y Culén frente a hongos fitopatógenos. *Bol. Latinoam. del Caribe Plantas Med. Aromáticas* 9, 212–215.

Hossen, J., Ali, M. A., and Reza, S. (2021). Theoretical investigations on the antioxidant potential of a non-phenolic compound thymoquinone: A DFT approach. *J. Mol. Model.* 27, 173. doi:10.1007/s00894-021-04795-0

Huang, D., Ou, B., and Prior, R. L. (2005). The chemistry behind antioxidant capacity assays. *J. Agric. Food Chem.* 53, 1841–1856. doi:10.1021/jf030723c

Humphrey, W., Dalke, A., and Schulten, K. (1996). Vmd: Visual molecular dynamics. *J. Mol. Graph.* 14 (33-8), 33–38. doi:10.1016/0263-7855(96)00018-5

Huxford, T., Huang, D.-B., Malek, S., and Ghosh, G. (1998). The crystal structure of the IκBα/NF-κB complex reveals mechanisms of NF-κB inactivation. *Cell.* 95, 759–770. doi:10.1016/s0092-8674(00)81699-2

Johnson, E. R., Keinan, S., Mori-Sánchez, P., Contreras-García, J., Cohen, A. J., and Yang, W. (2010). Revealing noncovalent interactions. *J. Am. Chem. Soc.* 132, 6498–6506. doi:10.1021/ja100936w

Karadag, A., Ozcelik, B., and Saner, S. (2009). Review of methods to determine antioxidant capacities. *Food Anal. Methods* 2, 41–60. doi:10.1007/s12161-008-9067-7

Larrazabal-Fuentes, M., Palma, J., Paredes, A., Mercado, A., Neira, I., Lizama, C., et al. (2019). Chemical composition, antioxidant capacity, toxicity and antibacterial activity of the essential oils from Acantholippia deserticola (Phil.) Moldenke (Rica rica) and Artemisia copa Phil. (Copa copa) extracted by microwave-assisted hydrodistillation. *Industrial Crops Prod.* 142, 111830. doi:10.1016/j.indcrop.2019.111830

Lountos, G. T., Jiang, R., Wellborn, W. B., Thaler, T. L., Bommarius, A. S., and Orville, A. M. (2006). The crystal structure of NAD(P)H oxidase from lactobacillus sanfranciscensis: Insights into the conversion of O2 into two water molecules by the flavoenzyme. *Biochemistry* 45, 9648–9659. doi:10.1021/bi060692p

Madhavi Sastry, G., Adzhigirey, M., Day, T., Annabhimoju, R., and Sherman, W. (2013). Protein and ligand preparation: Parameters, protocols, and influence on virtual screening enrichments. *J. Comput. Aided. Mol. Des.* 27, 221–234. doi:10.1007/s10822-013-9644-8

Malheiros, A., Filho, V. C., Schmitt, C. B., Santos, A. R. S., Scheidt, C., Calixto, J. B., et al. (2001). A sesquiterpene drimane with antinociceptive activity from Drimys winteri bark. *Phytochemistry* 57, 103–107. doi:10.1016/s0031-9422(00)00515-x

Miguel, M. G. (2010). Antioxidant activity of medicinal and aromatic plants. A review .*Flavour Fragr. J.* 25, 291–312. doi:10.1002/ffj.1961

MINSAL (2010). MINSAL, medicamentos herbarios tradicionales. Available at: https://www.minsal.cl/wp-content/uploads/2018/02/Libro-MHT-2010.pdf.

Monsálvez, M., Zapata, N., Vargas, M., Berti, M., Bittner, M., and Hernández, V. (2010). Antifungal effects of n-hexane extract and essential oil of Drimys winteri bark against Take-All disease. *Industrial Crops Prod.* 31, 239–244. doi:10.1016/j.indcrop.2009.10.013

Montenegro, I., Tomasoni, G., Bosio, C., Quiñones, N., Madrid, A., Carrasco, H., et al. (2014). Study on the cytotoxic activity of drimane sesquiterpenes and

nordrimane compounds against cancer cell lines. *Molecules* 19, 18993–19006. doi:10.3390/molecules191118993

Moon, J.-K., and Shibamoto, T. (2009). Antioxidant assays for plant and food components. *J. Agric. Food Chem.* 57, 1655–1666. doi:10.1021/jf803537k

Morris, G. M., Goodsell, D. S., Halliday, R. S., Huey, R., Hart, W. E., Belew, R. K., et al. (1998). Automated docking using a Lamarckian genetic algorithm and an empirical binding free energy function. *J. Comput. Chem.* 19, 1639–1662. doi:10.1002/(sici)1096-987x(19981115)19:14<1639::aid-jcc10>3.0.co;2-b

Muñoz, O., Christen, P., Cretton, S., Barrero, A. F., Lara, A., and Herrador, M. M. (2011). Comparison of the essential oils of leaves and stem bark from two different populations of drimys winteri a Chilean herbal medicine. *Nat. Product. Commun.* 6, 1934578X1100600. doi:10.1177/1934578x1100600630

Muñoz, O., Tapia-Merino, J., Nevermann, W., and San-Martín, A. (2021). Phytochemistry and biological properties of Drimys winteri JR et G. Forster var chilensis (DC) A. *Bol. Latinoam. del Caribe Plantas Med. Aromáticas* 20, 443–462. doi:10.37360/blacpma.21.20.5.33

Muñoz-Concha, D., Vogel, H., and Razmili, I. (2004). Variación de compuestos químicos en hojas de poblaciones de Drimys spp. (Magnoliophyta: Winteraceae) en Chile. *Rev. Chil. Hist. Nat.* 77, 43–50. doi:10.4067/s0716-078x2004000100005

Nararak, J., Giorgio, C. D., Sukkanon, C., Mahiou-Leddet, V., Ollivier, E., Manguin, S., et al. (2020). Excito-repellency and biological safety of β-caryophyllene oxide against *Aedes albopictus* and Anopheles dirus (Diptera: Culicidae). *Acta Trop.* 210, 105556. doi:10.1016/j.actatropica.2020.105556

Neira Ceballos, Z., Alarcón, A. M., Jelves, I., Ovalle, P., Conejeros, A. M., and Verdugo, V. (2012). Espacios ecológico-culturales en un territorio mapuche de la región de la araucanía en Chile. *Chungará (Arica)* 44, 313–323. doi:10.4067/s0717-73562012000200008

Paz, C., Cárcamo, G., Silva, M., Becerra, J., Urrutia, H., and Sossa, K. (2013). Drimendiol, A drimane sesquiterpene with quorum sensing inhibition activity. *Nat. Product. Commun.* 8, 1934578X1300800. doi:10.1177/1934578x1300800201

Pereira-Torres, D., Gonçalves, A. T., Ulloa, V., Martínez, R., Carrasco, H., Olea, A. F., et al. (2016). *In vitro* modulation of Drimys winteri bark extract and the active compound polygodial on *Salmo salar* immune genes after exposure to Saprolegnia parasitica. *Fish Shellfish Immunol.* 59, 103–108. doi:10.1016/j.fsi.2016.10.035

Perez, P., Ananias, R. A., and Hernandez, G. (2007). Estudio experimental del secado de renovales de canelo drimys winteri. *Maderas. Cienc. Tecnol.* 9, 59–70.

Pinchuk, I., Shoval, H., Dotan, Y., and Lichtenberg, D. (2012). Evaluation of antioxidants: Scope, limitations and relevance of assays. *Chem. Phys. Lipids* 165, 638–647. doi:10.1016/j.chemphyslip.2012.05.003

Rajan, V. K., and Muraleedharan, K. (2017). A computational investigation on the structure, global parameters and antioxidant capacity of a polyphenol, Gallic acid. *Food Chem.* 220, 93–99. doi:10.1016/j.foodchem.2016.09.178

Řezáč, J., and Hobza, P. (2012). Advanced corrections of hydrogen bonding and dispersion for semiempirical quantum mechanical methods. *J. Chem. Theory Comput.* 8, 141–151. doi:10.1021/ct200751e

Russo, A., Cardile, V., Graziano, A. C. E., Avola, R., Montenegro, I., Cuellar, M., et al. (2019). Antigrowth activity and induction of apoptosis in human melanoma cells by Drymis winteri forst extract and its active components. *Chemico-Biological Interact.* 305, 79–85. doi:10.1016/j.cbi.2019.03.029

Sanner, M. F. (1999). Python: A programming language for software integration and development. *J. Mol. Graph. Model.* 17, 57–61.

Satyal, P., Dosoky, N., Kincer, B., and Setzer, W. (2012). Chemical compositions and biological activities of Amomum subulatum essential oils from Nepal. *Nat. Product. Commun.* 7, 1934578X1200700. doi:10.1177/1934578x1200700935

Sharifi-Rad, J., Sureda, A., Tenore, G. C., Daglia, M., Sharifi-Rad, M., Valussi, M., et al. (2017). Biological activities of essential oils: From plant chemoecology to traditional healing systems. *Molecules* 22, 70. doi:10.3390/molecules22010070

Sharma, M., Grewal, K., Jandrotia, R., Batish, D. R., Singh, H. P., and Kohli, R. K. (2022). Essential oils as anticancer agents: Potential role in malignancies, drug delivery mechanisms, and immune system enhancement. *Biomed. Pharmacother.* 146, 112514. doi:10.1016/j.biopha.2021.112514

Sharma, V., Cantero-López, P., Yañez-Osses, O., and Kumar, A. (2018). Effect of cosolvents DMSO and glycerol on the self-assembly behavior of SDBS and CPC: An experimental and theoretical approach. *J. Chem. Eng. Data* 63, 3083–3096. doi:10.1021/acs.jced.8b00326

Skantar, A. M., Agama, K., Meyer, S. L., Carta, L. K., and Vinyard, B. T. (2005). Effects of geldanamycin on hatching and juvenile motility in *Caenorhabditis elegans* and *Heterodera glycines*. *J. Chem. Ecol.* 31, 2481–2491. doi:10.1007/s10886-005-7114-z

Stewart, J. J. P. (1990). MOPAC: A semiempirical molecular orbital program. *J. Comput. Aided. Mol. Des.* 4, 1–103. doi:10.1007/bf00128336

Stewart, J. J. P. (2007). Optimization of parameters for semiempirical methods V: Modification of NDDO approximations and application to 70 elements. *J. Mol. Model.* 13, 1173–1213. doi:10.1007/s00894-007-0233-4

Sudan, R., Bhagat, M., Gupta, S., Singh, J., and Koul, A. (2014). Iron (FeII) chelation, ferric reducing antioxidant power, and immune modulating potential of Arisaema jacquemontii (Himalayan Cobra Lily). *Biomed. Res. Int.* 2014, 1–7. doi:10.1155/2014/179865

Sundararajan, B., Sathishkumar, G., Seetharaman, P. k., Moola, A. K., Duraisamy, S. M., Mutayran, A. A. S. B., et al. (2022). Biosynthesized gold nanoparticles integrated ointment base for repellent activity against *Aedes aegypti* L. *Neotrop. Entomol.* 51, 151–159. doi:10.1007/s13744-021-00920-z

Tampe, J., Espinoza, J., Chacón-Fuentes, M., Quiroz, A., and Rubilar, M. (2020). Evaluation of drimys winteri (canelo) essential oil as insecticide against acanthoscelides obtectus (Coleoptera: Bruchidae) and aegorhinus superciliosus (Coleoptera: Curculionidae). *Insects* 11, 335. doi:10.3390/insects11060335

Touma, J., Navarro, M., Sepúlveda, B., Pavon, A., Corsini, G., Fernández, K., et al. (2020). The chemical compositions of essential oils derived from Cryptocarya alba and laurelia sempervirens possess antioxidant, antibacterial and antitumoral activity potential. *Molecules* 25, 5600. doi:10.3390/molecules25235600

Trott, O., Olson, A. J., and Vina, A. D. (2010). AutoDock Vina: Improving the speed and accuracy of docking with a new scoring function, efficient optimization, and multithreading. *J. Comput. Chem.* 31, 455–461. doi:10.1002/jcc.21334

Ultee, A., Bennik, M. H. J., and Moezelaar, R. (2002). The phenolic hydroxyl group of carvacrol is essential for action against the food-borne pathogen Bacillus cereus. *Appl. Environ. Microbiol.* 68, 1561–1568. doi:10.1128/aem.68.4.1561-1568.2002

Williams, P. A., Cosme, J., Ward, A., Angove, H. C., Matak Vinković, D., and Jhoti, H. (2003). Crystal structure of human cytochrome P450 2C9 with bound warfarin. *Nature* 424, 464–468. doi:10.1038/nature01862

Zapata, N., and Smagghe, G. (2010). Repellency and toxicity of essential oils from the leaves and bark of Laurelia sempervirens and Drimys winteri against *Tribolium castaneum*. *Industrial Crops Prod.* 32, 405–410. doi:10.1016/j.indcrop.2010.06.005

Zapata, N., Vargas, M., Medina, P., Viñuela, E., Rodriguez, B., and Fereres, A. (2010). The activity of a selected extract of Drimys winteri bark and polygodial on settling and probing behavior of the lettuce aphid Nasonovia ribisnigri. *Phytoparasitica* 38, 191–199. doi:10.1007/s12600-010-0087-7

Zapata, N., Vargas, M., Monsálvez, M., and Ceballos, R. (2011). Crude extracts of Drimys winteri bark to inhibit growth of Gaeumannomyces graminis var. tritici. *Chil. J. Agric. Res.* 71, 45–51. doi:10.4067/s0718-58392011000100006

Zhao, Y., and Truhlar, D. G. (2008). Exploring the limit of accuracy of the global hybrid meta density functional for main-group thermochemistry, kinetics, and noncovalent interactions. *J. Chem. Theory Comput.* 4, 1849–1868. doi:10.1021/ct800246v